Spreitzer, R. J., Jordan, D. B., & Ogren, W. L., (1982) *FEBS Lett. 148*, 117-121.
Tabita, F. R. (1988) *Microbiol. Rev. 52*, 155-189.
Tabita, F. R., & McFadden, B. A. (1974) *J. Biol. Chem. 249*, 3459-3464.
Tabita, F. R., & Small, C. L. (1985) *Proc. Natl. Acad. Sci. U.S.A. 82*, 6100-6103.
Valentin, K., & Zetsche, K. (1989) *Curr. Genet. 16*, 203-209.
van der Vies, S. M., Bradley, D., & Gatenby, A. A. (1986) *EMBO J. 5*, 2439-2444.
Voordouw, G., De Vries, P. A., Van den Berg, W. A. M., & De Clerk, E. P. J. (1987) *Eur. J. Biochem. 163*, 591-598.
Whitman, W., & Tabita, F. R. (1976) *Biochem. Biophys. Res. Commun. 71*, 1034-1039.
Yeoh, A., & Kitaoka, S. (1985) *Biochem. Biophys. Res. Commun. 131*, 1075-1079.

Analysis of the Two-State Behavior of the Thermal Unfolding of Serum Retinol Binding Protein Containing a Single Retinol Ligand†

Donald D. Muccio,*,‡ D. Vincent Waterhous,‡ Fred Fish,‡ and Christie G. Brouillette§
Department of Chemistry, University of Alabama at Birmingham, Birmingham, Alabama 35294, and Department of Organic Chemistry and Biochemistry Research, Southern Research Institute, Birmingham, Alabama 35205
Received September 3, 1991; Revised Manuscript Received March 19, 1992

ABSTRACT: Through the use of CD and DSC, the thermal unfolding of holo serum retinol binding protein containing a single, tightly bound retinol ligand was studied at pH 7.4. The DSC endotherm of the holoprotein ([retinol]/[protein] = 1) was asymmetric about the transition temperature of 78 °C. Using changes in ellipticity at 230 nm, the thermal unfolding curve was also asymmetric about the inflection point centered near 78 °C. van't Hoff enthalpies were determined by three means and compared to the calorimetric enthalpy (ΔH_{cal}) of 200 kcal/mol. A van't Hoff enthalpy of 190 kcal/mol was determined from the dependence of transition temperature on the concentration of the ligand-bound protein. This value agreed well with the van't Hoff enthalpies found from fits of the DSC (ΔH_{vH} = 184 kcal/mol) and spectroscopic (ΔH_{vH} = 181 kcal/mol) curves to a two-state thermodynamic model that included ligand dissociation (NR $\rightleftharpoons$ U + R, where NR is the native holoprotein, U is the unfolded apoprotein, and R is retinol). Poor agreement was obtained with a two-state model that ignored ligand dissociation (N $\rightleftharpoons$ U). Furthermore, the NR $\rightleftharpoons$ U + R model accounted for the asymmetry in both CD and DSC transitions and yielded a much improved fit of the data over the N $\rightleftharpoons$ U model. From these considerations and simulations on other equilibrium models, it is suggested that the NR $\rightleftharpoons$ U + R model is the simplest model that describes the thermal unfolding of this ligand-bound protein. Using an averaged van't Hoff enthalpy determined from fits of DSC and CD data, the cooperativity of this process was 0.925, indicating that the unfolding of the holoprotein is nearly two-state.

Due to the low water solubility of vitamin A, the biological actions of this vitamin are often mediated through the interactions with proteins (Blomhoff et al., 1990). Human serum retinol binding protein (SRBP)[1] is the vitamin A transport protein that is normally complexed to transthyretin (TTR) when charged with the vitamin (Peterson & Rask, 1971; Goodman, 1984; Blaner, 1989). The hydrophobic binding pocket within SRBP protects vitamin A from oxidation and at the same time minimizes the cytotoxic effects of this fat-soluble vitamin. SRBP is homologous to several proteins that are small hydrophobic molecule transporters including β-lactoglobulin, apolipoprotein D, α_1-microglobulin, α_1-acid glycoprotein, bilin binding protein, BG protein from olfactory epithelium, and others (Godovac-Zimmermann, 1988). Together these proteins form a new protein superfamily.

X-ray crystallography (Newcomer et al., 1984; Cowan et al., 1990) has revealed that SRBP (21 kilodaltons) contains a single globular domain with a 40-Å diameter. The protein has eight antiparallel β-sheets and one small segment of α-helix. The tertiary structure of the protein forms a β-barrel that is flattened at one end. Retinol is tightly bound (K_d = 7.5×10^{-8} M) to the protein by noncovalent interactions (Noy & Xu, 1990a) and is sandwiched in the center of the β-barrel. The trimethylcyclohexenyl ring of retinol is buried deep within the flattened portion of the protein. The polyene chain of retinol extends throughout the hydrophobic core of SRBP and is surrounded by several aromatic amino acids. The hydroxyl end group of retinol is close to the cleft of the protein near the external aqueous environment.

Most small, single-domain proteins unfold in a highly cooperative manner that can be best represented by a two-state equilibrium process without intermediates (Lumry et al., 1966; Privalov, 1979; Kim & Baldwin, 1982, 1990). Unfolding studies on single-domain proteins with noncovalently bound

†This research was supported by the National Institutes of Health (P01 CA 28103-08) and the National Science Foundation (DIR-8820511). D.V.W. was supported by a T32 training grant from the National Institutes of Health (EY07033-12).
*Address correspondence to this author.
‡University of Alabama at Birmingham.
§Southern Research Institute.

[1] Abbreviations: CD, circular dichroism; DSC, differential scanning calorimetry; SRBP, serum retinol binding protein; TTR, transthyretin; SDS-PAGE, sodium dodecyl sulfate-polyacrylamide gel electrophoresis; T_{max}, temperature of DSC maximum or inflection point in CD; T_m, temperature at which the equilibrium constant = 1; $T_{1/2}$, temperature at which the fraction of unfolded species = 0.5.

0006-2960/92/0431-5560$03.00/0

ligands are fewer in number, and these have usually addressed the problem of determining ligand binding constants (Schellman, 1975; Pace & McGrath, 1980; Schwarz, 1988; Brandts & Lin, 1990) and enthalpies (Manly et al., 1985; Edge et al., 1985). Only a few studies have determined the two-state nature of the unfolding process of proteins with noncovalently bound ligands. Sturtevant and co-workers (Fukada et al., 1983) have shown that arabinose binding protein in the presence of excess ligand unfolds in manner that is consistent with a simple $NL \rightleftharpoons U + L$ model, where L is the arabinose ligand. They conclude that the ligand has little effect on the unfolding of the rest of protein, besides the local ligand binding site. Schwarz (1988) has reached a similar conclusion for inhibitor binding to ribonuclease A. Each of these studies involved binding of a water-soluble ligand ($K_d = 10^{-2}$–10^{-6} M) to a cleft in the protein. Shrake and Ross (1988) have investigated fatty acid binding to multiple sites in human albumin, and have shown that the $N \rightleftharpoons U$ model accounts for the unfolding of the protein only when the ligand is in excess. Other studies by Sturtevant and co-workers (Manly et al., 1985; Edge et al., 1985) have involved more complicated equilibria of ligand binding to multiple domain proteins or protein complexes.

In this study, we investigate the thermal unfolding of holo-SRBP containing a retinol ligand bound to a single site in the protein. This hydrophobic ligand is bound more tightly than the other ligand complexes which have been studied, allowing for the unfolding process to be studied under conditions of limited apoprotein. Since the ligand is located in the interior of the protein, these studies will be able to evaluate the effects of a tightly bound ligand on the cooperativity of the thermal unfolding of this small, globular protein.

Materials and Methods

Protein Purification. Serum retinol binding protein was isolated from outdated human plasma following the method of Peterson (1971) with the following slight modifications. A 20 mM potassium phosphate buffer (KP), pH 7.4, was used throughout the purification (Muto et al., 1982). Prior to the first ion-exchange chromatographic step, the plasma was added to DEAE-A50 which was previously equilibrated in 200 mM NaCl in 20 mM KP buffer (pH 7.4), stirred by hand, and allowed to settle overnight. The supernatant of the suspension was discarded, and the DEAE-A50 resin containing at least 80% of the SRBP was packed in a column. The SRBP/TTR complex eluted with a 200–600 mM NaCl gradient after 24 h. Three other chromatographic steps followed: a G100 size-exclusion column in 1 M NaCl; a DEAE-A50 ion-exchange column with a 200–400 mM NaCl gradient; and a G100 size-exclusion column using as the eluant distilled water which was adjusted to pH 8 with NH_4OH. The SDS–PAGE (15%) of SRBP after the final G100 column contained a single band at 21 kDNa. The purified protein was stored at 4 °C in 20 mM KP, pH 7.4, with 150 mM NaCl and 0.02% sodium azide. The stored protein was charged with severalfold excess of *all-trans*-retinol in ethanol and chromatographed on a TTR affinity column (Vahlqusist et al., 1971), immediately prior to spectroscopic and DSC experiments.

Protein Concentration. Protein concentrations were determined by using radial immunodiffusion plates for the quantitation of SRBP (Behring Diagnostics; Somerville, NJ) and absorption spectroscopy using an ϵ_{280} of 46 mM^{-1} cm^{-1} (Heller & Horwitz, 1973). The absorption spectra were measured with either Perkin Elmer Lambda 6 or Aviv 14DS spectrophotometers, each of which was interfaced to a personal computer.

Circular Dichroism. The CD spectra were recorded with an AVIV 62DS spectropolarimeter interfaced to a personal computer (80386). Spectra were recorded on solutions containing 0.5–25 μM SRBP in 20 mM potassium phosphate (pH 7.4) and 150 mM NaCl. The CD spectra were measured every nanometer with 0.5-s averaging per point, and a 2-nm bandwidth. An 0.01-cm path-length cell was used for far-UV spectra. Spectra were signal-averaged by adding at least eight scans and base-line-corrected by subtracting a spectrum for the buffer obtained in an identical manner. Temperature was regulated with a Lauda RS2 circulating water bath, and the cell-holder temperature was measured with a thermosensor. A Bailey Instruments Bat 8 digital thermometer with a Sensortek thermistor was used to monitored the cell temperature. The thermal unfolding curves for SRBP were determined in the temperature mode at a single wavelength (230 nm) using a 3-nm bandwidth. Typically, a datum point was taken every 0.5 °C, and the signal was averaged 30 s. The temperature of the cell block was monitored, and these values were corrected for the differences between cell block and sample temperature.

Calorimetry. DSC experiments were performed with a Microcal MC-2 calorimeter (Amherst, MA) which contained matched tantalum cells. SRBP was first concentrated by Amicon ultrafiltration using a YM10 membrane filter and dialyzed with 20 mM potassium phosphate (pH 7.4) and 150 mM NaCl buffer. Equivalent volumes of sample and reference buffer were placed in their respective cells after deaerration at 20 mmHg for 15–30 min followed by purging with argon. DSC scans were run on samples that contained 15–35 μM SRBP with a 60 °C/h scan rate.

Calculations

The CD and DSC data were fit by a program written in BASIC (Microsoft). An alogrithum was developed to fit either of these data to thermodynamic models using the same optimization strategy. The heat capacities at each temperature, $C_p(T)$, from the DSC measurement were converted to calories per mole per degrees kelvin before analysis. The CD data at each temperature, $\theta(T)$, were analyzed in millidegrees. The program numerically integrates the DSC data to produce an enthalpy plot, $H(T)$ versus T, or numerically differentiates the CD data. In this manner, integrated DSC data can be compared to CD data while the DSC data are comparable to the first differences of the CD data (Sturtevant, 1974; Tiktopulo & Privalov, 1974).

The pre- and post-base-line temperature regions were chosen in the CD transition curve or the integrated DSC transition. The temperature dependence of $\theta_i(T)$ for the native (i = N) and unfolded (i = U) states in the pre- and posttransition region was determined by a linear least-squares fit. In a similar manner, the temperature dependence of the enthalpy, $H_i(T)$, of these species was found in the integrated DSC transition. This is summarized by eq 1 where $y_i(T)$ corresponds either

$$y_i(T) = y_i(0\ °C) + a_iT + b_iT^2;\ i = N \text{ or } U \qquad (1)$$

to the temperature-dependent ellipticity or to the temperature-dependent enthalpy of the native and unfolded species. The temperature dependence of the heat capacity of the N and U states, $C_p(T)$, in the DSC transition is found by differentiation of eq 1. The coefficients can be reoptimized for these data if desired. This usually leads to only small changes in the coefficients.

The thermal unfolding process can be described by two different thermodynamic models: a two-state process without ligand release ($N \rightleftharpoons U$) or with ligand release ($NR \rightleftharpoons U +$

R). For the N $\rightleftharpoons$ U process, the equilibrium constant is

$$K(T) = [U]/[N] = f_U/f_N \quad (2)$$

The fraction of unfolded species ($f_U = [U]/P_T$) in eq 2 is determined by

$$f_U = K(T)/[K(T) + 1] \quad (3)$$

For the NR $\rightleftharpoons$ U + R process, the equilibrium constant is given by

$$K(T) = [U][R]/[NR] \quad (4)$$

When the total retinol concentration, $R_T = [NR] + [R]$, is equal to the total protein concentration, $P_T = [NR] + [U]$, the equilibrium constant is

$$K(T) = P_T f_U^2/(1 - f_U) \quad (5)$$

which is the same as the equilibrium expression for the unfolding and dissociation of a protein dimer ($N_2 \rightleftharpoons U + U$) (Takahashi & Sturtevant, 1981). In contrast to the N $\rightleftharpoons$ U equilibrium (eq 2), the fraction of unfolded protein is dependent on the total protein concentration:

$$f_U = \{[K'(T)^2 + 4K'(T)]^{0.5} - K'(T)\}/2 \quad (6)$$

where $K'(T) = K(T)/P_T$.

The temperature dependence for the equilibrium constant, $K(T)$, includes heat capacity (ΔC_p) corrections to the van't Hoff enthalpy (ΔH_{vH}) and entropy (ΔS) changes (Schellman & Hawkes, 1980; Brandts & Lin, 1990):

$$\ln [K(T)/K(T_m)] = -[\Delta H_{vH}(T_m)/R](1/T - 1/T_m) + (\Delta C_p/R)[\ln (T/T_m) + T_m/T - 1] \quad (7)$$

where T_m is the temperature at which $K(T_m) = 1$. For the NR $\rightleftharpoons$ U + R equilibrium, the van't Hoff enthalpies (ΔH_{vH}) are reported at $T_{1/2}$ (temperature at which $f_U = 0.5$) using $\Delta H_{vH}(T) = \Delta H_{vH}(T_m) + \Delta C_p(T - T_m)$.

Initial guesses are made for $\Delta H_{vH}(T_m)$ and T_m, and the calculated ellipticies for CD data or calculated enthalpies for DSC data are determined at each temperature:

$$y_{calc}(T) = y_N(T) + [y_U(T) - y_N(T)]f_U \quad (8)$$

where f_U is determined by the choice of the model (eq 3 or 6). The calculated DSC curves are found by numerically differentiating the calculated enthalpy curves.

The $\Delta H_{vH}(T_m)$ and T_m values are adjusted through a modified Simplex procedure to yield the lowest sums of squares errors (SSE) between calculated and experimental values within the transition temperature region:

$$SSE = \sum\{y_{calc}(T) - y_{exp}(T)\}^2 \quad (9)$$

For the fits of CD data, the SSE was determined by differences in ellipticity, while the SSE for the DSC fits was determined by differences in heat capacity values. If desired, both thermodynamic parameters in eq 7 and the temperature coefficients in eq 1 could be optimized together for improved fits.

The change in heat capacity (ΔC_p) between the native and unfolded forms of the protein was determined by the difference between the pre- and post-base-line curves for the DSC data, and these were reported at $T_{1/2}$. The base line for the transition region in the DSC curve was adjusted between the pre- and post-base-line curves by the extent of reaction (Sturtevant, 1987). The calorimetric enthalpy (ΔH_{cal}) was determined by integration of the excess heat capacity of the transition, after base-line subtraction (Sturtevant, 1987).

The program was written to simulate either DSC or spectroscopic data. Synthetic DSC data were generated for a model that includes a ligand dissociation step, NR $\rightleftharpoons$ N + R (with equilibrium constant K_1), in equilibrium with a protein unfolding step, N $\rightleftharpoons$ U (with equilibrium constant K_2). This equilibrium model is abbreviated as NR $\rightleftharpoons$ N + R $\rightleftharpoons$ U + R within the text and does not mean to suggest an obligatory sequential mechanism. The equilibrium expressions for this model having an arbitrary total protein to total ligand ratio have been derived by Brandts and Lin (1990). Using a similar approach, we have derived the following equation when $R_T = P_T$ for the fraction of unfolded protein:

$$f_U = \{[[K'(T)^2 + 4K'(T)K_2(T)]/[1 + K_2(T)]]^{0.5} - K'(T)\}/2 \quad (10)$$

where $K(T) = K_1(T)K_2(T)$ and $K'(T) = K(T)/P_T$. The concentrations of the other species (f_N, f_{NR}, and f_R) are found through equilibrium expressions and/or mass balance equations. As N becomes less stable relative to NR and U [$K_2(T) \gg 1$], then eq 10 collapses to eq 6, indicating that the NR $\rightleftharpoons$ N + R $\rightleftharpoons$ U + R model approaches the NR $\rightleftharpoons$ U + R model.

When the equilibrium constant is dependent on protein concentration, the van't Hoff enthalpy can be determined from the change in $T_{1/2}$ on total protein concentration. Sturtevant and co-workers (Takahashi & Sturtevant, 1981; Fukada et al., 1983; Sturtevant, 1987) have derived a relationship for this dependence for the two-state unfolding of a multiple subunit protein with several ligands. For the NR $\rightleftharpoons$ U + R model with $P_T = R_T$, this expression is

$$\ln P_T = -[\Delta H_{vH}(T_0) - \Delta C_p T_0]/RT_{1/2} + (\Delta C_p/R) \ln (T_{1/2}/T_0) + \text{constant} \quad (11)$$

where T_0 is an arbitrary reference temperature.

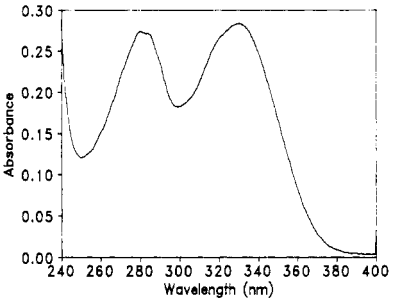

FIGURE 1: UV/vis absorption spectrum of SRBP in 20 mM KP (pH 7.4) and 150 mM NaCl at 25 °C.

Results

The near-UV absorption spectrum of SRBP at pH 7.4 is shown in Figure 1. The maximum at 278 nm is due mainly to aromatic amino acids of the protein while the 330-nm band is attributed to retinol. When the ratio of the 330- to 278-nm bands is 1.04, the protein is completely charged with the vitamin (Heller & Horwitz, 1973). This was typical of the spectra of the preparations reported within this study.

Differential Scanning Calorimetry. The DSC curve of SRBP at pH 7.4 is shown in Figure 2. A transition is centered near 78 °C. The endotherm from a second DSC scan was nearly identical to the first. This indicated that the refolding process is highly reversible (greater than 95% when the scan is stopped at 85 °C). However, the degree of reversibility decreased with exposure of the protein to temperatures greater than 85 °C for more than 10 min, suggesting that a slow irreversible event may occur at these temperatures.

The calorimetric enthalpy for the transition was calculated from the integration of the DSC data. First, the 55–65 °C

Table I: Thermodynamic Values Calculated from the DSC Endotherms and Far-UV CD Spectroscopic Thermal Unfolding Transitions of SRBP at pH 7.4[a]

model	ΔH_{cal} (kcal/mol)	ΔC_p [cal/(mol·K)]	T_{max} (°C)	ΔH_{vH} (kcal/mol)	$T_{1/2}$ (°C)	$\Delta H_{vH}/\Delta H_{cal}$	SSE
DSC analysis							
N ⇌ U	200	2570	78.0	125	77.48	0.625	29.71
NR ⇌ U + R	200	2530	78.0	181	77.28	0.905	6.68
CD analysis							
N ⇌ U		2500[b]	78.0[c]	120	77.27	0.600	101.16
NR ⇌ U + R		2500[b]	78.0[c]	184	77.43	0.920	10.75

[a] These data represent the typical values found from a single DSC and CD experiment (see Figures 2 and 3). The DSC experiments were repeated 5 times. The averaged values of ΔH_{cal} and ΔC_p were 200 ± 10 kcal/mol and 2500 ± 400 cal/(mol·K), respectively. The standard deviations for ΔH_{vH} and T_{max} were ±15 kcal/mol and ±0.4 °C, respectively. The CD experiments were repeated 7 times, and the fitted values had the same standard deviations as the DSC fits. [b] This values of ΔC_p was determined from the DSC studies and used in the fit of the CD data to N ⇌ U and NR ⇌ U + R models. [c] This value corresponds to the maximum in the first differences plot of the spectroscopic data.

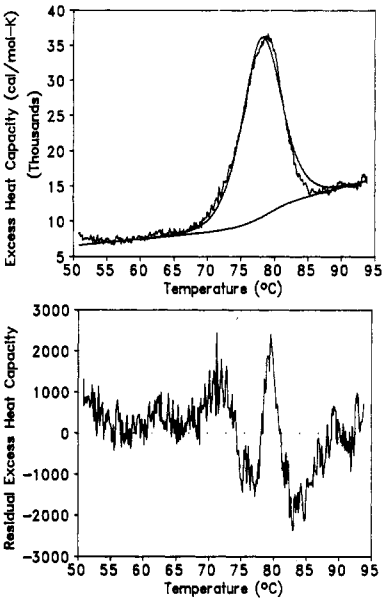

FIGURE 2: (Top) DSC endotherm of SRBP (23.2 μM) in 20 mM KP (pH 7.4) and 150 mM NaCl. The fitted curve (smooth line) utilized a two-state N ⇌ U model. (Bottom) Residual errors in excess heat capacity for the N ⇌ U fit of the DSC data.

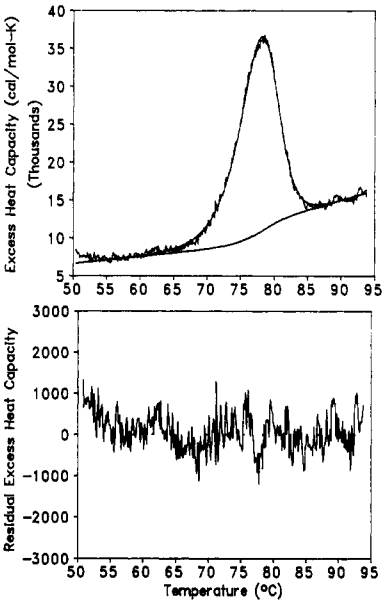

FIGURE 3: (Top) DSC endotherm of SRBP (23.2 μM) in 20 mM KP (pH 7.4) and 150 mM NaCl. The fitted curve (smooth line) utilized a two-state NR ⇌ U + R model. (Bottom) Residual errors in excess heat capacity for the NR ⇌ U + R fit of the DSC data.

and the 87–93 °C regions were chosen as the pre- and post-transitional base lines. The heat capacity base line for the transition region (65–85 °C) was adjusted between these limiting curves by the extent of the reaction (Sturtevant, 1987). After base-line subtraction, the excess heat capacity was integrated, and a calorimetric enthalpy of 200 kcal/mol was found (Table I). A calorimetric enthalpy of 200 ± 10 kcal/mol was found from an average of five measurements.

The van't Hoff enthalpy was obtained by fitting the DSC data to either of two thermodynamic models. The first model assumed that the thermal unfolding of the protein occurred without release of the ligand (N ⇌ U) while the second model included release of the ligand with unfolding (NR ⇌ U + R). For each model, the transition region (65–85 °C) was fit using the fixed pre- and posttransitional base lines chosen above. The thermodynamic parameters obtained from this initial fit were then used as input for the final optimization. The thermodynamic values were then optimized for the entire 55–90 °C region along with the temperature coefficients for the pre- and posttransitional base lines. The SSE for the fit of the data over the extended temperature region was only slightly better than the SSE calculated for the fit using fixed limiting curves. An estimate of the heat capacity change, ΔC_p, was also found by subtracting the pre- and posttransitional base lines at $T_{1/2}$ (Table I). From five measurements, ΔC_p was found to be 2500 ± 400 cal/(mol·K).

The best fit of the DSC data to the N ⇌ U model is shown in Figure 2. The fitted curve has a symmetrical shape (ignoring heat capacity changes) about a maximum temperature (T_{max}) of 77.5 °C. The maximum of the best-fitted curve is shifted by 0.5 °C to lower temperature than the experimental DSC curve maximum (Table I). The van't Hoff enthalpy determined from the fit of the data by this model was 125 kcal/mol, which is significantly less than the calorimetric enthalpy. In contrast, the fitted curves for the NR ⇌ U + R model has a T_{max} at 78.0 °C and a degree of asymmetry that closely matches the observed data (Figure 3). The van't Hoff enthalpy calculated from this model is 181 kcal/mol, which is in better agreement with the calorimetric value.

The closeness by which each model has fit the experimental data is best analyzed by viewing the residual error $[y_{exp}(T) - y_{calc}(T)]$. As shown in Figure 2, the residual error curve for the N ⇌ U model has a strong systematic trend due to the asymmetry of the experimental data relative to the symmetrical fitted curve. This systematic trend in the residual errors is largely reduced when a NR ⇌ U + R model is used to fit the data (Figure 3). This difference in fit is also reflected in the nearly 5-fold decrease in the SSE values of the NR ⇌ U + R fit to that of the N ⇌ U fit (Table I).

Thermally Induced Structural Changes of SRBP. Circular dichroism was used to determine the extent of structural change that occurs in the 78 °C DSC transition. The far-UV

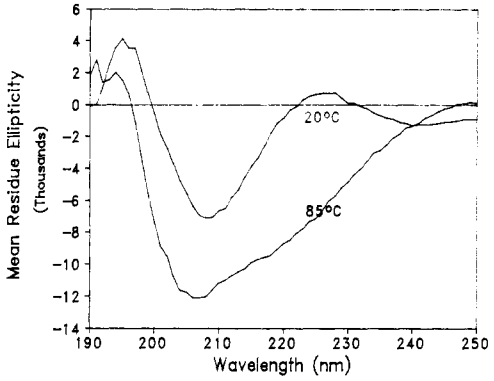

FIGURE 4: Far-UV CD spectra of SRBP in 20 mM KP (pH 7.4) and 150 mM NaCl at 20 and 85 °C. The path length was 0.01 cm.

Table II: Secondary Structure Predictions of SRBP from the CD Spectra at 20 and 85 °C[a]

method	wavelength region (nm)	% α-helix	% β-sheet	% β-turn	% random coil
X-ray[b]		8	51	15	26
CD (20 °C)	190–240	0	83	0	17
	190–210	14	47	12	27
CD (85 °C)	190–240	20	20	14	46
	190–210	27	0	22	51

[a] Secondary structure analysis by the method of Chang et al. (1978). [b] Analysis of the X-ray structure at 2.0-Å resolution by Cowan et al. (1984).

CD spectrum of SRBP at pH 7.4 and 20 °C is shown in Figure 4. Positive bands occur at both 195 and 227 nm, a negative band at 209 nm, and crossover points at 192, 200, and 230 nm in the 20 °C spectrum. The far-UV spectrum of SRBP was reported previously by others only to 200 nm (Gotto et al., 1972; Rask et al., 1972; Heller & Horwitz, 1973). There is reasonable agreement in this region between the spectra reported previously and the spectrum presented here. The 85 °C spectrum of SRBP at pH 7.4 is also shown in Figure 4. A large change occurs in this spectrum compared to the 20 °C spectrum primarily in the 220–230-nm region and the 195-nm band. When the sample was cooled to 20 °C, the cooled spectrum was identical to the spectrum prior to heating.

The secondary structure of SRBP was analyzed at both 20 and 85 °C by the method of Yang and co-workers (Chang et al., 1978). A large amount of β-sheet secondary structure was predicted from the analysis of the 20 °C spectrum of SRBP between 190 and 240 nm (Table II). This is consistent with the eight β-strands found in the X-ray structure (Newcomer et al., 1984), but it overestimates the abundance by almost 2-fold. An examination of the fit shows that it agrees best with the data between 190 and 210 nm. A fit of 190–210-nm region of the CD data yields estimates of secondary structure that are in much closer agreement to the values obtained from X-ray diffraction. Goodman and co-workers (Gotto et al., 1972) analyzed the CD data only between 200 and 240 nm and found a much lower β-sheet content (22%). This may be attributed to the low information content of the β-structure in this spectral region (Woody, 1985; Johnson, 1988) and possible complications due to aromatic residues (Manning & Woody, 1987). The secondary structure of SRBP at 85 °C was determined from both the 190–210-nm and 190–240-nm regions. A large conformational change is found regardless of the region analyzed. Nearly all the β-sheet content is lost with a substantial increase occurring in the random-coil content.

Thermal Unfolding of SRBP Using CD Spectroscopy. In an effort to correlate the structural changes observed in the CD spectrum with the DSC transition, CD spectroscopy was used to monitor the thermal unfolding of SRBP at 230 nm (Figure 5). The unfolding curve had an inflection point near 78 °C which is similar to the maximum in the DSC curve. The spectrum of the cooled sample was nearly identical to the spectrum prior to heating (at least 95% recovery of signal).

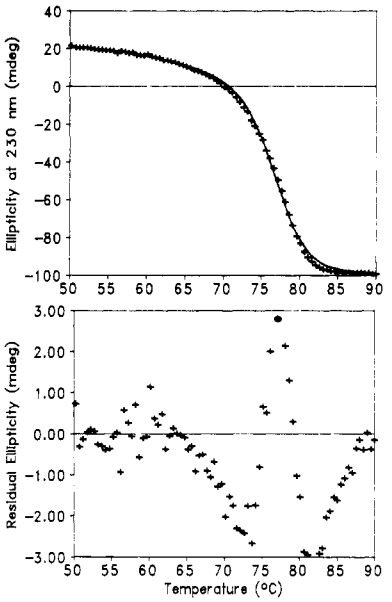

FIGURE 5: (Top) Thermal unfolding of SRBP (15 μM) monitored by CD at 230 nm (+++). The thermodynamic fit of the CD data to a N ⇌ U model (smooth line). (Bottom) Residual errors in ellipticity for the N ⇌ U fit of the CD data.

In order to obtain van't Hoff enthalpies, the ellipticity at 230 nm versus temperature was fit to N ⇌ U and NR ⇌ U + R models. The procedure used to fit the spectroscopic data was similar to the method used to fit the DSC data. The pretransitional region (55–65 °C) was fit to a quadratic dependence on temperature (Tiktopulo & Privalov, 1974). The posttransitional base line (87–90 °C) was fit only to a linear dependence. After the transition region (65–85 °C) was fit to either thermodynamic model, the 55–90 °C region was completely optimized for the best values of the thermodynamic values and base-line fits.

The results of these fits are shown in Table I. The residual error in the N ⇌ U fit to the CD data was very systematic (Figure 5), and these trends were similar to the residuals found from the fit of the DSC data with this model (Figure 2). When a NR ⇌ U + R model was used, most of the systematic deviation was eliminated (Figure 6). This better fit of the data with the dissociative model is also reflected in the 10-fold reduction in SSE (Table I). The van't Hoff enthalpy determined for the N ⇌ U model (120 kcal/mol) was much less than that determined for the NR ⇌ U + R model (184 kcal/mol). This relationship in van't Hoff enthalpies was also found from the fits of the DSC data (Table I).

The NR ⇌ U + R model fit the DSC and spectroscopic data significantly better than the N ⇌ U model. If the dissociative model is applicable, one would expect the unfolding temperature to be dependent on the total concentration of the ligand-bound protein (see eq 11), while a N ⇌ U model is concentration-independent. A study was undertaken on the effects of the concentration of the holoprotein complex ($R_T = P_T$) on the temperature of unfolding. The thermal unfolding curves were monitored by CD spectroscopy at 230 nm. As shown in Table III, the T_{max} values (first differences) systematically increased with increasing concentration of the protein–ligand complex. This is additional evidence in support

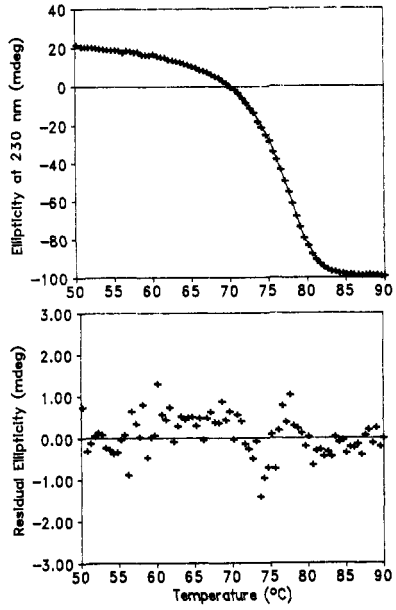

FIGURE 6: (Top) Thermal unfolding of SRBP (15 μM) monitored by CD at 230 nm (+++). The thermodynamic fit of the CD data to a NR $\rightleftharpoons$ U + R model (smooth line). (Bottom) Residual errors in ellipticity for the NR $\rightleftharpoons$ U + R fit of the CD data.

Table III: Thermodynamic Analyses[a] of the Unfolding of SRBP by Monitoring the Ellipticity at 230 nm at Several Concentrations of Total Protein

P_T (μM)	T_{max} (°C)	$T_{1/2}$ (°C)	ΔH_{vH} (kcal/mol)
0.52	76.6	75.62	170
2.97	78.1	77.52	179
4.86	78.4	77.88	181
7.86	79.2	78.65	210
13.05	79.7	79.15	189
22.0	80.6	80.01	187
24.3	81.3	80.58	195

[a] Values obtained from the NR $\rightleftharpoons$ U + R fit of the data. The mean ΔH_{vH} for these seven fits was 187 $\pm$ 13 kcal/mol.

of a the NR $\rightleftharpoons$ U + R model over a N $\rightleftharpoons$ U model. The data were fit to a NR $\rightleftharpoons$ U + R model to determine the $T_{1/2}$ values as a function of concentration. The van't Hoff enthalpy was then determined from the concentration dependence of $T_{1/2}$ using eq 11 with a heat capacity change of 2.5 kcal/(mol·K) (Table I). The plot of ln P_T versus $1/T_{1/2}$ is given in Figure 7 for the data of the NR $\rightleftharpoons$ U + R fits shown in Table III. The van't Hoff enthalpy at 77.3 °C is 190 kcal/mol. This value is in good agreement with the van't Hoff enthalpies derived from the thermodynamic fits of the spectroscopic (184 kcal/mol) and DSC (181 kcal/mol) data using the NR $\rightleftharpoons$ U + R model.

Discussion

The two-state model seems to be a reasonable approximation of the reversible unfolding of single-domain proteins. As reviewed by Privalov (1979), DSC has provided a quantitative measure of the two-state model for several proteins. It was shown that the van't Hoff enthalpy agreed well ($\Delta H_{vH}/\Delta H_{cal}$ = 0.95) with the calorimetric enthalpy (Privalov & Khechinashvili, 1974) as expected for a model that excludes appreciable formation of stable intermediates. Even though there are many exceptions to the two-state hypothesis (Privalov, 1982), these proteins tend to contain multidomains or have large, complicated structures.

In this study, we have investigated holo-SRBP containing a single, noncovalently bound molecule of retinol. Even though

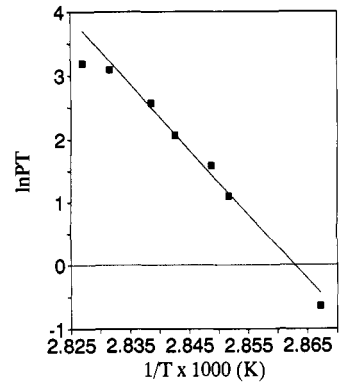

FIGURE 7: $T_{1/2}$ dependence on the total concentration of ligand-bound protein (P_T). The data between 2.97 and 22 μM (Table III) were fit to eq 11 using ΔC_p = 2.5 kcal/(mol·K) (Table I). The ΔH_{vH} was 190 $\pm$ 13 kcal/mol at 77.3 °C.

this ligand is only a small fraction of the total molecular weight of the protein, it is long and has noncovalent contacts with many residues within the protein (Cowan et al., 1990). In fact, the vitamin is buried between two antiparallel β-sheets in the interior of the protein and divides the protein in half. One may wonder if the vitamin allows communication between these hydrophobic regions of structure to the extent that this protein behaves as a single cooperative unit (Sandberg & Terwilliger, 1989). The most direct approach to study this effect is to use the calorimetric test for cooperativity, as was done with other single-domain proteins without ligands. However, prior to answering the question concerning this two-state nature of the unfolding process, it was necessary to establish the appropriate model for data analysis.

We have studied the thermal unfolding of this protein under the conditions of complete saturation of the ligand site, but without excess ligand (R_T/P_T = 1). We have shown that the thermal unfolding curves monitored by DSC and CD are asymmetric about the midpoint of the transition. When a two-state model (N $\rightleftharpoons$ U) was used, the fitted curve did not adequately account for the asymmetry, even including heat capacity changes. The T_{max} of the fitted curve was consistently 0.5 °C less than the observed value. Furthermore, ΔH_{vH} evaluated from this model was only 60% of the observed ΔH_{cal}. Furthermore, this ΔH_{vH} value is in poor agreement with the ΔH_{vH} determined from the dependence of $T_{1/2}$ on the concentration of the holoprotein complex (R_T/P_T = 1).

To a good approximation, we have shown that a two-state model that takes into account the release of ligand with unfolding (NR $\rightleftharpoons$ U + R) addresses many of the shortcomings of the N $\rightleftharpoons$ U model. The asymmetry in the thermal unfolding data is accounted for by the dissociative model. The systematic errors in the residuals plot are significantly reduced when either DSC or CD data are fit by this model. The T_{max} of the fitted curves agreed well with the experimental data. The ΔH_{vH} determined from the fit of the DSC and CD data to this model agreed well with the ΔH_{vH} found from the concentration dependence of $T_{1/2}$. Takahashi and Sturtevant (1981) have shown similar trends for a related system. The asymmetric thermal unfolding of a subtilisin inhibitor dimer was fit much better by a $N_2 \rightleftharpoons 2U$ model than a N $\rightleftharpoons$ U model. Even though the equilibria describing the unfolding of a protein with ligand release (NR $\rightleftharpoons$ U + R) or with dimer dissociation (N_2 $\rightleftharpoons$ U + U) are similar, it has not been well recognized in the literature.

The average ΔH_{vH} value determined at $T_{1/2}$ from the fits of the DSC (five) and CD (eight) experiments by the NR $\rightleftharpoons$ U + R model is 185 $\pm$ 6 kcal/mol. The cooperativity of the

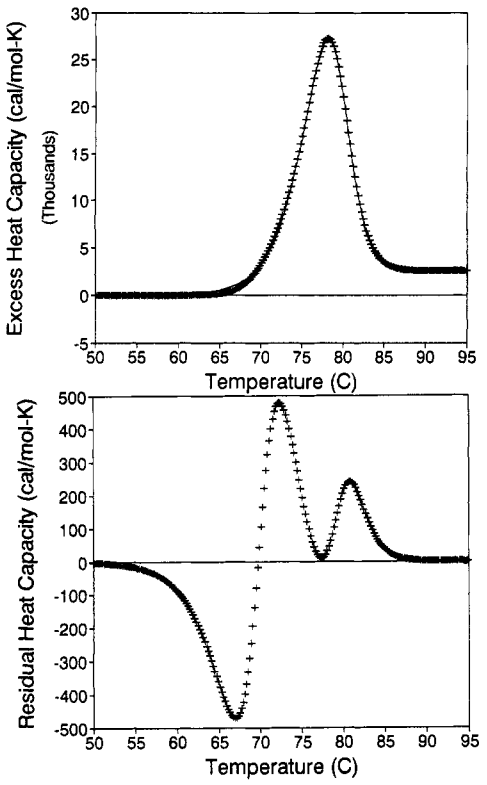

FIGURE 8: (Top) Simulated DSC curve (+++) based on the NR ⇌ N + R ⇌ U + R model ($R_T = P_T = 23.2$ μM) using $\Delta H_{vH}(T_m) = 0$ and $\Delta S(T_m) = -32.6$ cal/(mol·K) for the NR ⇌ N + R reaction, and $\Delta H_{vH}(T_m) = 163$ kcal/mol, $\Delta S(T_m) = 474.6$ cal/(mol·K), $T_m = 70.3$ °C, and $\Delta C_p = 2.53$ kcal/(mol·K) for the N + R ⇌ U + R reaction. The calorimetric enthalpy was 200 kcal/mol. Best-fitted curve (solid) to the simulated data using a NR ⇌ U + R model ($R_T = P_T = 23.2$ μM) with $\Delta H_{vH}(T_m) = 218$ kcal/mol, $\Delta S(T_m) = 597.5$ cal/(mol·K), and $\Delta C_p = 2.53$ kcal/(mol·K). The $\Delta H_{vH}(T_{1/2})$ was 181 kcal/mol for the fitted curve. (Bottom) Residual errors in heat capacity (calories per mole per degrees kelvin) for the NR ⇌ U + R fit of the simulated DSC data. Note that the vertical scale of the bottom plot has been reduced by 35.

thermal unfolding process ($\Delta H_{vH}/\Delta H_{cal}$) was determined to be 0.925. This value is quite close to that found for proteins that do not contain ligands (Privilov, 1979). This ratio indicates that the thermal unfolding of holo-SRBP is also nearly two-state and the accumulation of thermodynamically stable intermediates is small, analogous to other single-domain proteins without ligands.

Several studies (Manly et al., 1985; Robert et al., 1988; Shrake & Ross, 1990; Brandts & Lin, 1990) have shown that an equilibrium model which includes a ligand dissociation step in equilibrium with the thermal unfolding process (in the simplest form, a NR ⇌ N + R ⇌ U + R model) accounts for the changing features of the DSC curves with different ligand/protein ratios. We have generated simulated DSC data using the NR ⇌ N + R ⇌ U + R equilibrium model ($R_T = P_T = 23.2$ μM). For the protein in the absence of ligand,[2] the transition temperature was 70.3 °C with an enthalpy change of 163 kcal/mol and a ΔC_p of 2.53 kcal/(mol·K). A temperature-independent equilibrium constant ($K_d = 7.5 \times 10^{-8}$ M at 25 °C) was used for the ligand dissociation equilibrium (Noy & Xu, 1990a,b). The simulated DSC curve generated by the NR ⇌ N + R ⇌ U + R model ($R_T/P_T = 1$) is a single, asymmetric transition centered near 78.2 °C (Figure 8, top). This curve is very similar to the experimental DSC curve of holo-SRBP (Figure 2).

The simulated DSC curve generated by the NR ⇌ N + R ⇌ U + R model was fit by the NR ⇌ U + R model. The simulated DSC curve was fit well by the NR ⇌ U + R model using an $\Delta H_{vH} = 181$ kcal/mol at $T_{1/2} = 77.3$ °C and $\Delta C_p = 2.53$ kcal/(mol·K) (solid curve in Figure 8, top). A small deviation in the fit occurs around 70 °C. This is most apparent in the residual errors plot[3] (Figure 8, bottom). This difference is due to the N ⇌ U transition in the simulated DSC data. However, the N ⇌ U transition is small since the population of N is low in this temperature region. (Note the reduction by 35 in the y axis of the bottom plot in Figure 8.) This is in agreement with eq 6 and 10 (Calculations), which show that the f_U predicted by the NR ⇌ U + R model approaches that for the NR ⇌ N + R ⇌ U + R model when the the population of N approaches zero.

Most of the studies on the thermal unfolding of ligand-bound proteins have centered on the use of DSC to determine ligand binding enthalpies and binding constants (Pace & McGrath, 1980; Fukada et al., 1983; Schwartz, 1988; Brandts & Lin, 1990). We are also interested in determining binding constants and binding enthalpies for retinol and other synthetic analogs to SRBP; however, this requires a thermodynamic analysis of the holoprotein in the presence of different concentrations of ligands (preferably) as well as a complete study on the apoprotein. Current effort has been placed on the isolation of an apo form of the protein that is capable of regeneration with retinol and complete recovery of the thermodynamic properties of holo-SRBP presented in this paper.

In summary, we have shown that the thermal unfolding of holo-SRBP is a highly cooperative process. The tight packing of the hydrophobic ligand in the protein binding site is apparently effective enough to bridge the two halves of the protein, resulting in nearly two-state unfolding. The two-state model (NR ⇌ U + R) that involves ligand release with protein unfolding is the simplest model to describe this thermal process.

ACKNOWLEDGMENTS

We are grateful to both reviewers for helpful comments. Reviewer 2 was especially helpful with the analysis of the data presented in Figure 8.

Registry No. Retinol, 68-26-8.

REFERENCES

Blaner, W. S. (1989) *Endocr. Rev. 10*, 308–316.
Blomhoff, R., Green, M. H., Berg, T., & Norum, K. R. (1990) *Science 250*, 399–404.
Brandts, J. F., & Lin, L.-N. (1990) *Biochemistry 29*, 6927–6940.
Chang, C. T., Wu, G.-S. C., & Yang, J. T. (1978) *Anal. Biochem. 91*, 13–31.
Cowan, S. W., Newcomer, M. E., & Jones, T. A. (1990) *Proteins: Struct., Funct., Genet. 8*, 44–61.
Edge, V., Allewell, N. M., & Sturtevant, J. M. (1985) *Biochemistry 24*, 5899–5906.
Fukada, H., Sturtevant, J. M., & Quichjo, F. A. (1983) *J. Biol. Chem. 258*, 13193–13198.

[2] No experimental thermodynamic information is available on apo-SRBP. These values were chosen for the N ⇌ U equilibrium in the NR ⇌ N + R ⇌ U + R model to produce a DSC curve with a T_{max} near 78 °C which is experimentally observed (Table I).

[3] The residual errors centered near 81 °C (Figure 8, bottom) are a consequence of the inability of the NR ⇌ U + R model to fit the simulated DSC data near 70 °C. When simulated DSC data are generated with smaller K_d so the N ⇌ U transition is smaller and separated more from the NR ⇌ U + R transition, the residual errors in the fit of the NR ⇌ U + R model are nearly zero (unpublished results).

Godovac-Zimmermann, J. (1988) *Trends Biochem. Sci. 13*, 64–66.
Goodman, D. S. (1984) in *The Retinoids* (Sporn, M. B., Roberts, A. B., & Goodman, D. S., Eds.) Vol. 2, pp 42–82, Academic Press, New York.
Gotto, A. M., Lux, S. E., & Goodman, D. S. (1972) *Biochem. Biophys. Acta 271*, 429–435.
Heller, J., & Horwitz, J. (1973) *J. Biol. Chem. 248*, 6308–6316.
Johnson, W. C. (1988) *Annu. Rev. Biophys. Biophys. Chem. 17*, 145–155.
Kim, P. S., & Baldwin, R. L. (1982) *Annu. Rev. Biochem. 51*, 459–489.
Kim, P. S., & Baldwin, R. L. (1990) *Annu. Rev. Biochem. 59*, 631–660.
Lumry, R., Biltonen, R., & Brandts, J. F. (1966) *Biopolymers 4*, 917–944.
Manly, S. P., Matthews, K. S., & Sturtevant, J. M. (1985) *Biochemistry 24*, 3842–3846.
Manning, M. C., & Woody, R. W. (1987) *Biopolymers 26*, 1731–1752.
Muto, Y., Shidoji, Y., & Kanda, Y. (1982) *Methods Enzymol. 81*, 840–852.
Newcomer, M. E., Jones, T. A., Aqvist, J., Sundelin, J., Eriksson, U., Rask, L., & Peterson, P. A. (1984) *EMBO J. 3*, 1451–1454.
Noy, N., & Xu, Z. J. (1990a) *Biochemistry 29*, 3878–3883.
Noy, N., & Xu, Z. J. (1990b) *Biochemistry 29*, 3888–3892.
Pace, C. N., & McGrath, T. (1980) *J. Biol. Chem. 255*, 3862–3865.
Peterson, P. A. (1971) *J. Biol. Chem. 246*, 34–43.
Peterson, P. A., & Rask, L. (1971) *J. Biol. Chem. 246*, 7544–7550.
Privalov, P. L. (1979) *Adv. Protein Chem. 33*, 167–241.
Privalov, P. L. (1982) *Adv. Protein Chem. 35*, 1–104.
Privalov, P. L., & Khechinashvili, N. N. (1974) *J. Mol. Biol. 86*, 665–684.
Rask, L., Peterson, P. A., & Bjork, I. (1972) *Biochemistry 11*, 264–268.
Roberts, C. H., Gill, S. J., & Wyman, J. (1988) *Biochemistry 27*, 6829–6835.
Sandberg, W. S., & Terwilliger, T. C. (1989) *Science 245*, 54–57.
Schellman, J. A. (1975) *Biopolymers 14*, 999–1018.
Schellman, J. A., & Hawkes, R. B. (1980) in *Protein Folding* (Jaenicke, R., Ed.) pp 331–343, Elsevier/North-Holland Biomedical Press, New York.
Schwarz, F. P. (1988) *Biochemistry 27*, 8429–8436.
Shrake, A., & Ross, P. D. (1988) *J. Biol. Chem. 263*, 15392–15399.
Shrake, A., & Ross, P. D. (1990) *J. Biol. Chem. 265*, 5055–5059.
Sturtevant, J. M. (1974) *Annu. Rev. Biophys. Bioeng. 3*, 35–51.
Sturtevant, J. M. (1987) *Annu. Rev. Phys. Chem. 38*, 463–488.
Takahashi, K., & Sturtevant, J. M. (1981) *Biochemistry 20*, 6185–6190.
Tiktopulo, E. I., & Privalov, P. L. (1974) *Biophys. Chem. 1*, 349–357.
Vahlquist, A., Nilson, S. F., & Peterson, P. A. (1971) *Eur. J. Biochem. 20*, 160–168.
Woody, R. W. (1985) *Peptides (N.Y.) 7*, 15–114.

Picosecond Dynamics of Bacteriorhodopsin, Probed by Time-Resolved Infrared Spectroscopy†

Rolf Diller,‡ Mark Iannone,‡ Benjamin R. Cowen,‡ Sudipta Maiti,§ Roberto A. Bogomolni,‖ and Robin M. Hochstrasser*,‡

Department of Chemistry and Department of Biochemistry and Biophysics, University of Pennsylvania, Philadelphia, Pennsylvania 19104, and Department of Chemistry, University of California, Santa Cruz, California 95064

Received January 21, 1992; Revised Manuscript Received March 24, 1992

ABSTRACT: The photoinduced reaction cycle of bacteriorhodopsin (BR) has been studied by means of a recently developed picosecond infrared spectroscopic method at ambient temperature. BR – K difference spectra between 1560 and 1700 cm^{-1} have been recorded at delay times from 100 ps to 14 ns. The spectrum remains unchanged during this period. The negative difference OD band at 1660 cm^{-1} indicates the peptide backbone responds within 50 ps. A survey in the region of carboxylic side chain absorption around 1740 cm^{-1} reveals that perturbations of those groups, present in low-temperature FTIR spectra, are not observable within 10 ns, suggesting a slow conformational change.

Bacteriorhodopsin is the single protein in the purple membrane of *Halobacterium halobium* (Oesterhelt & Stoeckenius, 1973) and is widely studied as a model system for light to energy-transducing proteins and transmembrane ion pumps. It contains a retinal chromophore which is bound to the lysine-216 residue via a protonated Schiff base (SB). Absorption of a photon in the visible leads to a reaction cycle, during which the BR_{570}, J_{625}, K_{610}, L_{550}, M_{412}, N, and O_{640} states (subscript, approximate absorption maximum) of the protein are generated with time constants in the range from hundreds of femtoseconds to milliseconds (Lozier et al., 1975; Zinth et al., 1988; Mathies et al., 1988) and during which protons are pumped across the cell membrane. The generated chemical potential enables the bacterium to produce ATP under

† This research was supported by the NIH and the NSF.
‡ Department of Chemistry, University of Pennsylvania.
§ Department of Biochemistry and Biophysics, University of Pennsylvania.
‖ Department of Chemistry, University of California.

0006-2960/92/0431-5567$03.00/0